STEADY AND UNSTEADY RANSE SIMULATIONS FOR PLANING CRAFTS

Rodrigo Azcueta, MTG Marinetechnik, Hamburg [1]

SUMMARY

This paper presents steady and unsteady free-surface RANSE simulations for a power boat sailing at extremely high speeds up to $F_n = 4$. The steady flow computations efficiently yield the complete resistance curve in one go – from zero to maximum boat speed – instead of computing only for one boat speed at the time. The dynamic sinkage and trim are also computed along with the resistance for the whole F_n-range. The simulations of boat motions in waves aim to show that the method is robust enough and well suited for simulating the large amplitude boat's responses to incident waves, also in the planing condition, whereby the boat experiences regular and irregular jumps in the waves. The results of the simulations in waves are compared with model tests performed at the towing tank of the Osaka Prefecture University and with computations by Söding based on an extention of Wagner's theory. With CPU times of a few hours on a small cluster of personal computers for each characteristic wave, the RANSE simulations promise great potential for the near future.

1. INTRODUCTION

For any vessel sailing at a high F_n, like power boats, the change in the boat's running attitude (sinkage, trim, heel) due to the pressure field around the hull is quite significant so that its effects influence performance to a large extent and should be taken into account.

In this work, a general approach was implemented, extending a Navier-Stokes code to couple the fluid flow with the body motions induced by the flow and/or by external forces. This allows not only to compute dynamic sinkage and trim but also to simulate the unsteady boat motions in the 6 DOF. The methodology has been applied to several dynamic cases showing that large amplitude motions including capsizing, slamming, water entry, wave-piercing and water on deck can be simulated. The robustness of this methodology is mainly due to the simplicity of tracking the vessel's motions without deforming the numerical mesh or using complicated multi-mesh strategies. The VOF method in conjunction with a moving, rigid mesh attached to the vessel and suitable boundary conditions are shown to be very robust and efficient. In this work, only the application of this methodology to planing crafts, with the additional difficulty of the extremely high Froude numbers up to $F_n = 4$, will be demonstrated.

2. NUMERICAL METHOD

To couple the fluid flow and body motions I extended the Navier-Stokes solver COMET with a *body-motion module*. COMET is a commercial code developed in Germany by ICCM GmbH, now a member of the CD Adapco Group, the developers of the well-known multi-purpose STAR-CD code.

The general idea for coupling the fluid flow with the body motions is as follows: the Navier-Stokes flow solver computes the flow around the body in the usual way, taking into account the fluid viscosity, flow turbulence and deformation of the free surface. The forces and moments acting on the body are then calculated by integrating the normal (pressure) and tangential (friction) stresses over the body surface. Following this, the body-motion module solves the equations of motion of the rigid body in the 6 DOF using the forces and moments calculated by the flow solver as input data. The motion accelerations, velocities and displacements (translations and rotations) are obtained by integrating in time. The position of the body is updated and the fluid flow is computed again for the new position. By iterating this procedure over the time, the body trajectory is obtained.

2.1 BODY-MOTION MODULE

Two orthogonal Cartesian reference systems (RS) are used: A non-rotating, non-accelerating Newtonian RS (O, X, Y, Z) which moves forward with the mean ship speed, and a body-fixed RS (G, x, y, z) with origin at G, the centre of mass of the body. The undisturbed free-surface plane always remains parallel to the XY plane of the Newtonian RS. The Z-axis points upwards. The x-axis of the body-fixed RS is directed in the main flow direction, i.e. from bow to stern, the y-axis is taken positive to starboard and the z-axis is positive upwards. The body motions are executed using a *single-grid strategy*, where a rigid, body-fixed grid moves relative to the Newtonian RS, and the ficticious flow forces due to the grid movement are automatically taken into account in the flow equations. The body-motion module is linked and run simultaneously

[1] azcueta@mtg-marinetechnik.de, rodrigo@azcueta.net

with the flow solver and can operate and update all flow variables, boundary conditions and parameters of the numerical method.

The motion of the rigid body in the 6 DOF are determined by integrating the equations of variation of linear and angular momentum written in the form referred to G (all vector components expressed in the Newtonian RS):

$$m\ddot{\vec{X}}_G = \vec{F} \quad , \quad \overline{\overline{T}}\,\overline{\overline{I}}_G\overline{\overline{T}}^{-1}\dot{\vec{\Omega}} + \vec{\Omega} \times \overline{\overline{T}}\,\overline{\overline{I}}_G\overline{\overline{T}}^{-1}\vec{\Omega} = \vec{M}_G \tag{1}$$

where m is the body mass, $\ddot{\vec{X}}_G$ the absolute linear acceleration of G, $\vec{F}$ is the total force acting on the body, $\dot{\vec{\Omega}}$ and $\vec{\Omega}$ are the absolute angular acceleration and angular velocity, respectively, and $\vec{M}_G$ is the total moment with respect to G, $\overline{\overline{I}}_G$ is the tensor of inertia of the body about the axes of the body-fixed RS, $\overline{\overline{T}}$ is the transformation matrix from the body-fixed into the Newtonian RS.

The contributions to the total force and to the total moment acting on G are:

$$\vec{F} = \vec{F}_{flow} + \vec{W} + \vec{F}_{ext} \quad , \quad \vec{M}_G = \vec{M}_{G_{flow}} + (\vec{X}_{ext} - \vec{X}_G) \times \vec{F}_{ext} \tag{2}$$

where $\vec{F}_{flow}$ and $\vec{M}_{G_{flow}}$ are the total fluid flow force and moment determined by integrating the normal (pressure) and tangential (friction) stresses, obtained from the Navier-Stokes solver. They include the static and the dynamic components of the water and of the air flow. $\vec{W}$ is the body weight force. $\vec{F}_{ext}$ can be any external force acting on the body which one wants to introduce to simulate for instance the towing forces and moments.

The boat motions are described in each time instant by the position of its centre of gravity $\vec{X}_G$ and the body orientation given by $\overline{\overline{T}}$. Surge, sway and heave are defined in this work as the translations of G in the directions of the Newtonian RS. The angles of rotation are defined in the following order: First the rotation around the vertical axis in the Newtonian RS (yaw or leeway angle), second the rotation around the new transverse axis (pitch or trim angle), and last the rotation around the new longitudinal axis (roll or heel angle). To integrate in time the equations of motion a first-order explicit discretisation method has shown to work well and is used preferably. Instead of integrating the angular velocity $\vec{\Omega}$ to obtain the rotation angles, the new orientation of the body is found by integrating the unit vectors of the body-fixed RS, which are the columns of $\overline{\overline{T}}$. For details on the body-motion module see [1].

2.2 FLOW SOLVER

The solution method in COMET is of finite-volume-type and uses control volumes (CVs) with an arbitrary number of faces (unstructured meshes). It allows cell-wise local mesh refinement, non-matching grid blocks, and moving grids with sliding interfaces. The integration in space is of second order, based on midpoint rule integration and linear interpolation. The method is fully implicit and uses quadratic interpolation in time through three time levels.

The deformation of the free surface is computed with an *interface-capturing scheme* of VOF type (Volume Of Fluid), which has proven to be well suited for flows involving breaking waves, sprays, hull shapes with flat stern overhangs and section flare, etc. In this method, the solution domain covers both the water and air region around the hull and both fluids are considered as one effective fluid with variable properties. An additional transport equation for a void fraction of liquid is solved to determine the interface between the two fluids. The *High-Resolution-Interface-Capturing* (HRIC) discretisation scheme for convective fluxes in the void fraction equation is used to ensure the sharpness of the interface.

The solution method is of pressure-correction type and solves sequentially the linearised momentum equations, the continuity equation, the conservation equation of the void fraction, and the equations for the turbulence quantities. The linear equation systems are solved by conjugate gradient type solvers and the non-linearity of equations is accounted for by Picard iterations. The method is parallelised by domain decomposition in both space and time and is thus well suited for 3-D flow computation with free surfaces – especially when they are unsteady, as in the case of freely-floating bodies – since they require a lot of memory and computing time. For details on the flow solver see [3].

2.3 PREVIOUS APPLICATIONS AND VALIDATION

Calculations with this method including the dynamic sinkage and trim (steady-state case) were validated for the Series 60 hull and for the model of a very fat ship with a blunt bow similar to a tanker (breaking-wave computations). These two examples showed that the method works well for very tiny changes in sinkage, trim (and also heel for the drift sailing condition) as well as for very large ones. The inclusion of the dynamic sinkage and trim in the calculations improved the agreement with experiments, and thus performance prediction.

Simulations of unsteady body motions were validated for 2-D drop tests with a wedge (used for slamming investigations). Comparisons with experiments proved very good agreement for both magnitude and timing of the accelerations, velocities and motions [1]. A validation for a 3-D case was also carried out for the model of a naval combatant in head waves and 2

DOF (heave and pitch) and showed good agreement with experiments. Slamming and green water on deck were simulated as well. In all these simulations the body trajectory, velocity and accelerations are obtained from the flow forces and/or external forces acting on the body without the need for prescribing the body trajectory.

The method has also been extensively applied to the steady flow around sailing yachts and for the simulation of the yachts responses to incident waves coming from any direction [2]. Furthermore, investigations of the dynamics of very large container vessels (up to 360 m length) sailing in extremely shallow water have been carried out (results to be published).

2.4 NUMERICAL MESH AND SIMULATION SET-UP

The model used for this investigations is a 1/4-scale model of a personal watercraft used for extensive studies in the towing tank of Osaka Prefecture University, [4]. Its main dimensions are shown in Table I and its body plan in Figure 1.

Table I. Model data

lenght L_{oa}	0.625 m	breath B	0.250 m
lenght L_{pp}	0.600 m	draft d	0.059 m
depth D	0.106 m	mass m	4.28 kg
deadrise β	22°		
KG	0.111 m	LCG-transom	0.285 m

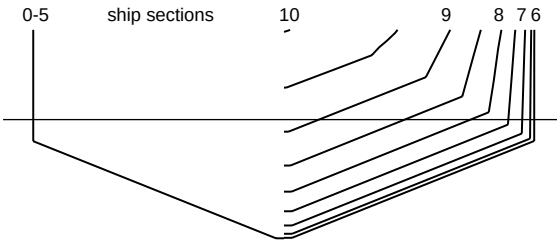

Figure 1. Body plan of planing craft model

Four grids of different resolutions and size of computational domain were used to assess the influence of these parameters. The grids were generated using the ICEM-CFD Hexa mesh generator. The coarsest grid had around 95 000 and the finest one 230 000 CVs for one boat side (symmetry plane at the centre-line plane). Even the finest grid is still a bit too coarse in front of the model, in the wake and in transversal direction. Good resolution is achieved around the hull and in free-surface region. The differences in forces and motions as computed on the three grids were not very large, so that in the following only the results for the finest grid will be presented. The computational domain for the finest grid extends for about $1.5\ L_{oa}$ in front of the bow, $3.75\ L_{oa}$ behind the transom, $0.65\ L_{oa}$ above deck, $1.9\ L_{oa}$ below the keel and $1.9\ L_{oa}$ to the side. The mesh has such a large domain, specially above the deck, to allow large pitch motions in head waves. The CVs are mainly aligned to a water plane taking into account an average trim angle of $4.0\ °$. Figure 2 shows the mesh

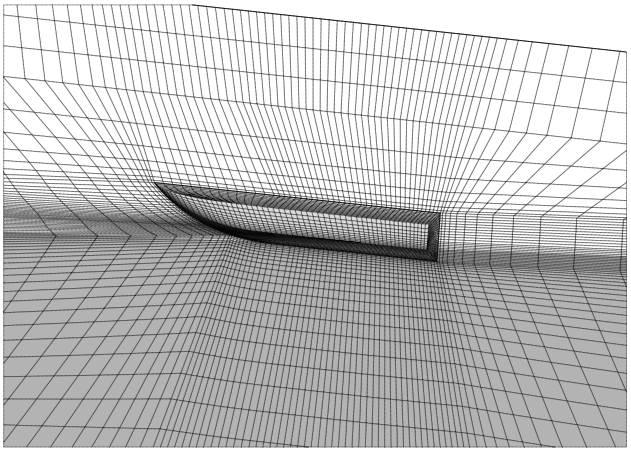

Figure 2. Numerical mesh around hull viewed from de side

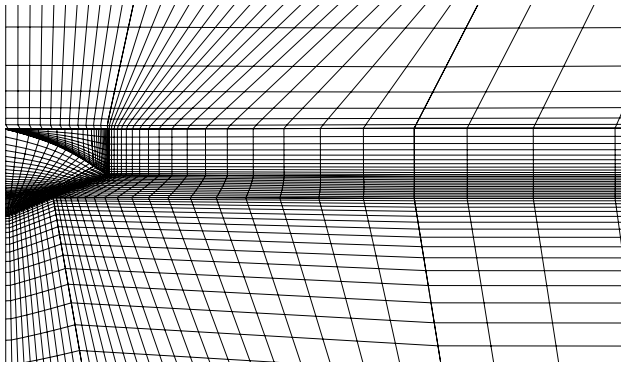

Figure 3. Numerical mesh around hull viewed from the front

around the hull viewed from the side and slightly from the front and below and Figure 3 shows the mesh on the hull and a transverse mesh surface viewed from the front. The mesh shown in the figures is the second finest. The finest grid was obtained after a local mesh refinement in longitudinal direction in front of the model. This refinement was necessary to avoid numerical problems with the incident waves due to highly stretched cells in longitudinal direction.

The pitch radius of gyration, not known from the experiments, was estimated to be $k_{yG} = 0.2\ L_{oa}$. The front, side, bottom and top flow-boundaries were specified as an inlet of constant known velocity (boat speed in opposite direction plus orbital velocity of the incoming waves) and known void fraction distribution defining the water and air regions (wave elevation). The wake flow-boundary was specified as a zero-gradient boundary of known pressure distribution (hydrostatic pressure). All calculations were performed using the standard k-ϵ turbulence model with wall functions (R_n: $1.8 \cdot 10^6$ to $5.6 \cdot 10^6$).

3. RESISTANCE TESTS

RANSE computations are usually carried out for a given boat speed at a time and then repeated for as many speeds as are of interest. Here, a different approach is used: the entire resistance curve is computed in one single run. To achieve this, the boat, starting from the position at rest or sailing at a low constant speed, accelerates very slowly until it reaches the maximum boat speed expected. Since the acceleration is small and the flow basically converges for each instant boat speed, the calculation can be considered to be quasi-steady. Note that although the flow is steady once converged, since the free surface has to develop its final wave pattern, the computations (single-speed or accelerating) have to be carried out iterating in time, i.e. solving the transient terms of the flow equations.

Figure 4 shows the resistance test computed accelerating the boat from 2 m/s to 9 m/s (F_n-range from 0.8 to 4.04). The solid line represents the resistance curve. As mentioned earlier, a very important feature of these computations is that the dynamic sinkage and trim are computed throughout the entire F_n-range. These curves are given in Figure 4 as well (dashed and dotted lines respectively). The fat dots also shown in Figure 4 represent the results for the single-speed runs for $v_o = 2, 3, 4, 5, 6, 7, 8, 9$ and 10 m/s. The agreement with the resistance test calculation is good with exception of the trim angle for $F_n = 1.2$ (3 m/s).

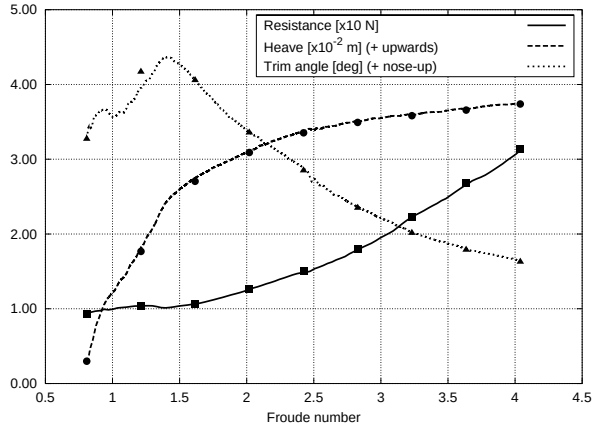

Figure 4. Numerical resistance test and computations at constant speeds

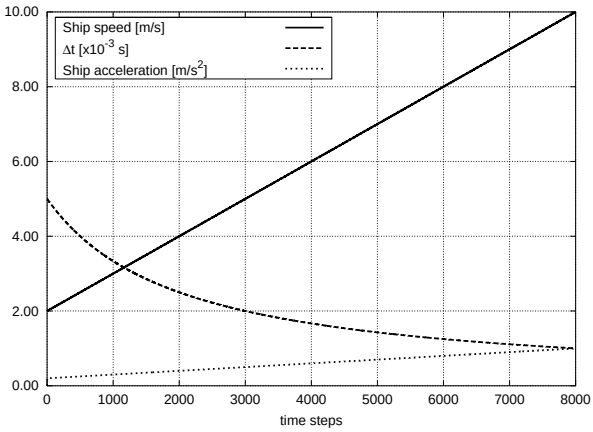

Figure 5. Curve shapes for boat speed, acceleration and Δt

The CPU time needed for computing the resistance curve over the entire F_n-range is obviously greater than when computing only one boat speed, but it pays off if many boat speeds are to be computed. 25 hrs CPU on linux-cluster using 3 AMD 2000+ processors were needed to simulate the resistance curve of Figure 4. The CPU time for computing one single speed was about 8 hrs using one AMD 2000+ processor ($1{,}000$ time steps). That means that about 10 single speeds could have been computed in the time needed to compute the whole resistance curve. The resistance curve for the entire F_n-range was computed performing $8{,}000$ time steps, cf. Figure 5, and since for each time step the boat speed has changed, $8{,}000$ different boat speeds were computed.

One important issue to take into account when performing these kind of resistance tests is to ensure that a constant *Courant Number* $c = v\Delta t/\Delta x$ is used for the entire F_n-range. A value of $c < 0.5$ seems to be appropriate. The Courant Number is the ratio of the time step size Δt to the characteristic convection time, $v/\Delta x$, the time required for a disturbance to be convected a distance Δx. Since the mesh resolution giving Δx remains unchanged for the entire F_n-range and v is changing (the boat accelerates), Δt should the suited accordingly. This is achieved in these computations by setting $\Delta t = \Delta x_o/v$ or a minimum value for Δt when v tends to zero. Here Δx_o is a characteristic CV length, which is given as input at the beginning of the simulation.

The next issue to consider is that if a constant acceleration is used, in the high speed range where a small Δt is required, the boat's speed would change very slowly requiring too many time steps to reach the desired maximum speed. This is solved by gradually increasing the acceleration with increasing speed. The resulting curve shapes for Δt, acceleration and boat speed are given in Figure 5 as a function of the time step.

If the boat acceleration is small enough, the additional forces due to the added mass are negligible. In that case the single-speed run and the numerical resistance test will yield the same results for a given speed, as is confirmed in Figure 4 with the exception of the trim angle for 3 m/s. Furthermore, the same results should be obtained if the boat were decelerating from maximum to minimum speed. This test was also performed using inverted function shapes for acceleration and Δt. The results of the resistance test in 'decelerating mode' overlap with the lines in Figure 4 with exception of a small F_n-range between 0.8 and 1.4.

4. BOAT IN INCIDENT WAVES

This work is based on prior simulations of ship responses to incident waves coming from different directions. However, F_n in the prior simulations was moderate ($F_n < 0.5$). The obtained results were quite encouraging; some results could be successfully validated with model tests and others, for which no model tests were available, showed plausible qualitative results. Large amplitude motions including capsizing were simulated, [2]. Also the occurrence of slamming and water on deck was simulated and animated by video sequences.

The challenge the present simulations constitute, however, results from the high F_n, which introduces numerical difficulties in the generation of the incident waves, since the mean flow velocity due to the boat forward speed is 2 to 3 orders of magnitude larger than the orbital velocity of the waves. Special care is to be taken in the selection of aspect ratios of CVs to avoid unphysical wave irregularities.

The incident waves are generated at the inlet flow-boundary by imposing the instantaneous wave elevation and orbital velocities according to the linear wave theory. The orbital velocities of the waves are thus superimposed on the mean flow velocity. Three wave parameters are set at the beginning of a simulation: The wave amplitude ζ_w, the wave length λ_w and the wave direction μ relative to the boat course ($\mu = 0^\circ$ means from astern and $\mu = 90^\circ$ from port). Due to numerical diffusion the wave amplitude hitting the boat is reduced to some extent, although the used VOF-method produces surprisingly good results on relatively coarse meshes.

Figure 6 shows a snap-shot during a simulation at an instant when the boat is completely in the air after jumping in an oblique wave. The figure shows the edges of the computational domain. Also shown is the cut of the computational domain with the undisturbed waterplane. In the single-grid strategy used in these simulations, the computational domain moves as a whole relative to this plane. The boundary conditions – the mean flow velocity, the orbital velocity, the void fraction distribution defining the wave elevations, the turbulence parameters and so on – have to be very carefully imposed at each time instant relative to the undisturbed waterplane. The VOF method and the implemented boundary conditions have proven to be very robust, since the free surface can leave the computational domain in any place, i.e. through the top flow-boundary in case that the boat heels or pitches with a large angle. Even the simulation of capsizing upside down is possible.

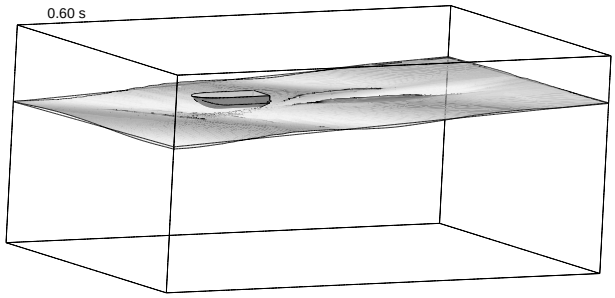

Figure 6. Power boat model jumping in oblique waves at 9 m/s

4.1 VALIDATION OF MOTIONS

Figures 7 and 8 show the motions and forces for the boat sailing at 9 m/s in head waves of 0.02 m height and 3.5 m length. Shown is also the start of the simulation: since the wave length is large in this case and the motions highly damped the motions are already periodic after 3 to 4 periods. These simulation were performed over $4{,}000$ time steps with a time-step size $\Delta t = 0.0005$ s and 5 iterations per time step. The CPU time needed for this simulation was 33 hours on one AMD 2000+ processor or 8.5 hrs on 4 processors.

The time histories of motions and forces shown in the last figures are typical for all the simulations. However, depending on boat speed and the ratios of wave length to boat length and wave height to boat draft, the motions show sinusoidal character, not-sinusoidal periodical character with motion periods of 1, 2 or 3 times the wave encounter period, or even chaotic non-periodic character. Above certain boat speed and wave steepness the boat jumps completely out of the water. Simulations in oblique waves including the roll angle and in head waves with the boat free to surge in the waves assuming a constant drive force were also performed but will not be presented here due to lack of space.

The results of these simulations are compared with experiments by *Katayama et al.* [4] performed at the towing tank of the Osaka Prefecture University and with computations by *Söding* [5] based on an extention of Wagner's theory. Figures 9 and 10 show respectively the non-dimensional heave and pitch for the boat sailing at 9 m/s ($F_n = 3.6$) in head waves of 0.02 m height for varying wave lengths. The heave, measured at the centre of mass of the model G, was made non-dimensional by dividing the maximum minus the minimum heave amplitude $\zeta_{max} - \zeta_{min}$ by the wave height $H_w = 2\zeta_w$. The pitch angle was made non-dimensional by dividing the maximum minus the minimum pitch angle $\theta_{max} - \theta_{min}$ by the (linear) wave slope double amplitude kH_w where k is the wave number. In all the simulations of Figures 9 and 10, since the waves are relatively long and flat, the responses are periodic with the wave encounter period. The comparison shows in general a slight improvement in prediction by the RANSE simulations compared to the Wagner-type method although both fail to predict the peak motion by $\lambda_w / L_{oa} = 5.6$.

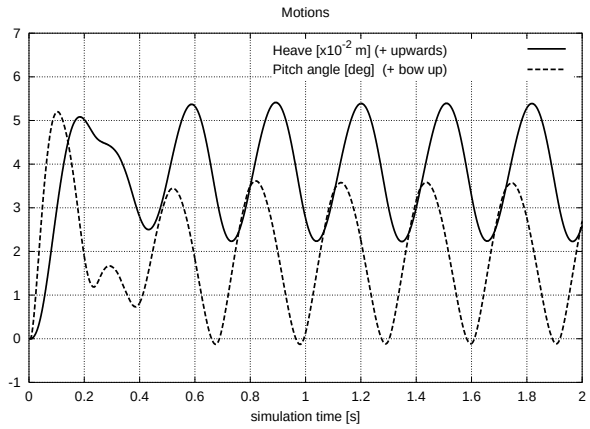

Figure 7. Motions for $F_n = 3.6$, $\mu = 180°$, $H_w = 0.02$ m and $\lambda_w = 3.5$ m. ($T_e = 0.309$ s)

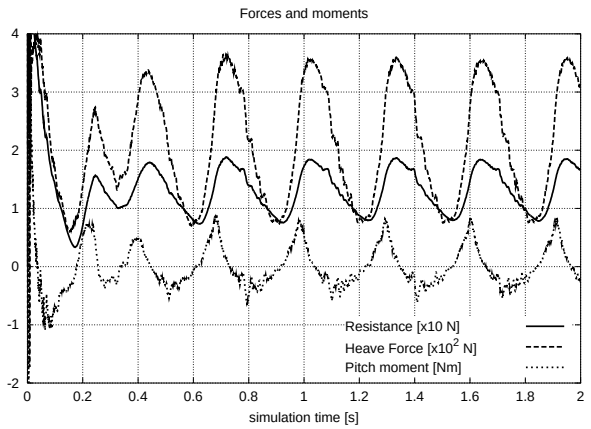

Figure 8. Forces and moments for $F_n = 3.6$, $\mu = 180°$, $H_w = 0.02$ m and $\lambda_w = 3.5$ m

Sources for uncertainties in these simulations of motions in waves are the guessed pitch radius of gyration and the reduction in wave height encountered by the boat due to numerical diffusion. The latter tends to reduce the predicted non-dimensional values. On the other side, to perform experiments at such high speeds with a quite small model represents in principle a big challenge. Difficulties arise for measuring small angles and displacements, for producing regular waves in the tank and for measuring transient motions – which depend to some extent on the initial conditions – in a very short period of time. The latter also apply to the simulations, since the motions responses may i.e. switch from single-period to double-period of wave encounter after a time span which is too large for RANSE simulations. In this case the motion amplitude would change substantially. All these aspect may be deteriorating the agreement of results.

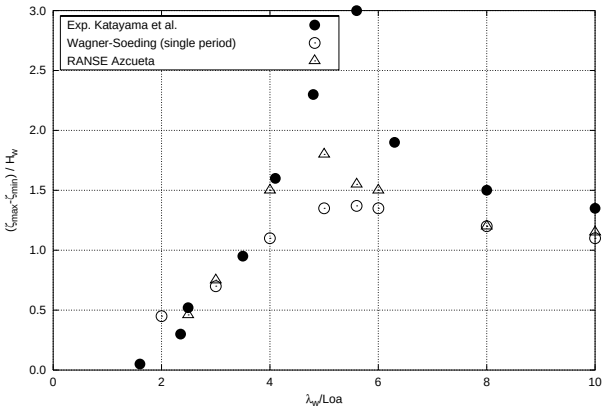

Figure 9. Non-dimensional heave over non-dimensional wave length for $H_w = 0.02$ m and $F_n = 3.6$

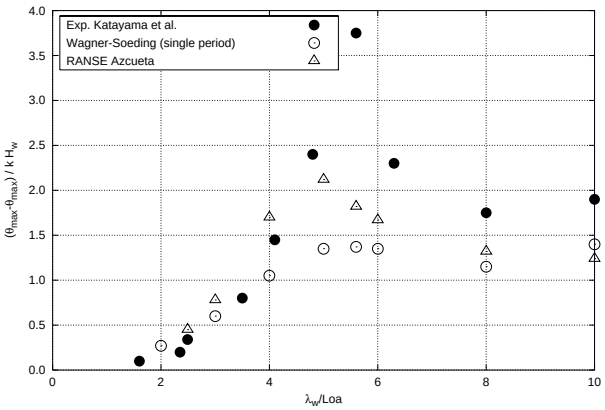

Figure 10. Non-dimensional pitch over non-dimensional wave length for $H_w = 0.02$ m and $F_n = 3.6$

References

[1] Azcueta, R., *"Computation of Turbulent Free-Surface Flows Around Ships and Floating Bodies"*, PhD. thesis, Technical University Hamburg-Harburg, 2001.

[2] Azcueta, R., *"RANSE simulations for sailing yachts including dynamic sinkage & trim and unsteady motions in waves"*, High Performance Yacht Design Conference Auckland, 2002.

[3] Ferziger, J. H. & Perić, M., *Computational Methods for Fluid Dynamics*, Springer, Berlin, 1996.

[4] Katayama, T., Hinami, T. & Ikeda, Y., "Longitudinal motion of a super high-speed planing craft in regular head waves", *4th Osaka Colloquium on Seakeeping Performance of Ships*, 2000.

[5] Caponnetto, M., Söding, H. & Azcueta, R., "Motion Simulations for Planing Boats in Waves", *Ship Technology Research*, to be published 2003.